



## Volume generation towards dynamic surface morphing in liquid crystal polymer networks

Danqing Liu

To cite this article: Danqing Liu (2016) Volume generation towards dynamic surface morphing in liquid crystal polymer networks, *Liquid Crystals*, 43:13-15, 2136-2143, DOI: [10.1080/02678292.2016.1195898](https://doi.org/10.1080/02678292.2016.1195898)

To link to this article: <https://doi.org/10.1080/02678292.2016.1195898>



© 2016 The Author(s). Published by Informa UK Limited, trading as Taylor & Francis Group.



Published online: 16 Jun 2016.



Submit your article to this journal [↗](#)



Article views: 798



View related articles [↗](#)



View Crossmark data [↗](#)



Citing articles: 10 View citing articles [↗](#)

## Volume generation towards dynamic surface morphing in liquid crystal polymer networks

Danqing Liu

Group Functional Organic Materials & Devices (SFD), Department of Chemical Engineering & Chemistry, Eindhoven University of Technology, AZ 5612 Eindhoven, the Netherlands

### ABSTRACT

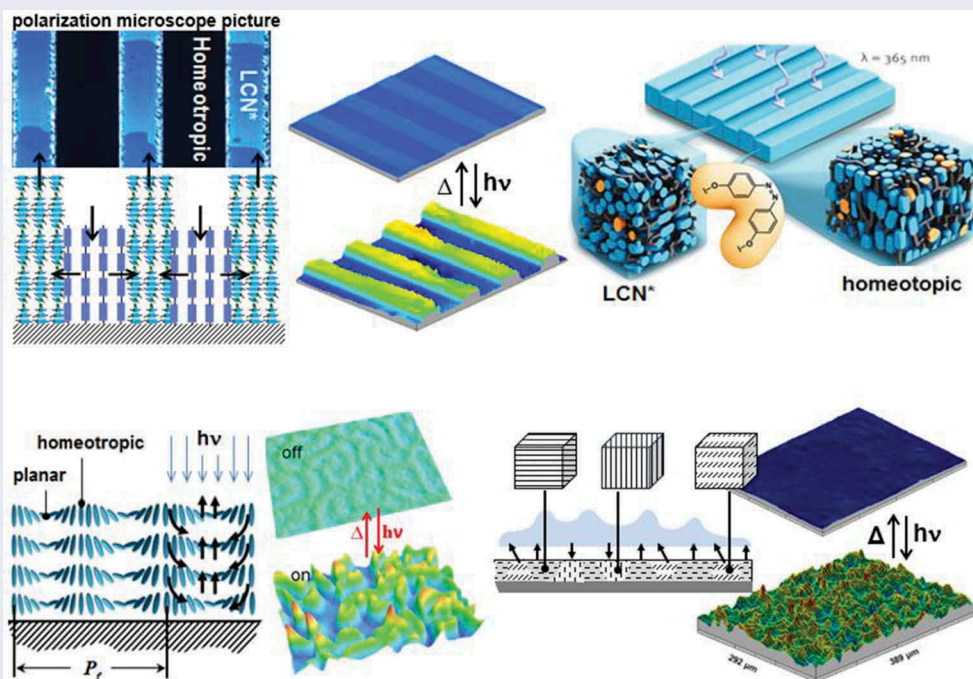
Thin coatings based on liquid crystal networks (LCNs) modified with azobenzene moieties are able to create dynamic surface topographies in the micrometre range by exposure with UV light. The surface corrugations can be erased and restored by switching 'off' and 'on' the UV illumination. Various configurations were presented. The formation of the protrusions was proven to be induced mainly by excessive volume formation when the order in the LCNs is reduced. It is suggested that this extra volume formation can be further enhanced by stimulating the oscillatory dynamics of *trans-cis* and *cis-trans* isomerisation. Therefore, dual-wavelength exposure not only exciting the *trans* state of azobenzene by 365 nm UV light but simultaneously also the *cis* state by 455 nm blue light was shown to enhance the effect.

### ARTICLE HISTORY

Received 29 April 2016

### KEYWORDS



Dynamic surface topographies; liquid crystal networks; volume increase; azobenzene



### Introduction

The ability to switch the coating surface between a flat state to the pre-designed corrugated state by an external trigger might lead to many new applications or might improve existing ones. For instance, in microfluidics mixing is substantially enhanced by the existence of microscopic topographic structures on the channel

surface. Active control over those topographies enables switching between a mixing and a non-mixing state [1]. Also tribology-related properties such as friction, adhesion/release can be altered by topographic changes. Tribological alterations are especially important for applications in motion control and haptics, for example, for robotic manipulation and as touch-input devices [2–4]. Besides the mechanical properties, the

**CONTACT** Danqing Liu  [D.liu1@tue.nl](mailto:D.liu1@tue.nl)  Group Functional Organic Materials & Devices (SFD), Department of Chemical Engineering & Chemistry, Eindhoven University of Technology, Eindhoven AZ 5612, the Netherlands

© 2016 The Author(s). Published by Informa UK Limited, trading as Taylor & Francis Group.

This is an Open Access article distributed under the terms of the Creative Commons Attribution-NonCommercial-NoDerivatives License (<http://creativecommons.org/licenses/by-nc-nd/4.0/>), which permits non-commercial re-use, distribution, and reproduction in any medium, provided the original work is properly cited, and is not altered, transformed, or built upon in any way.

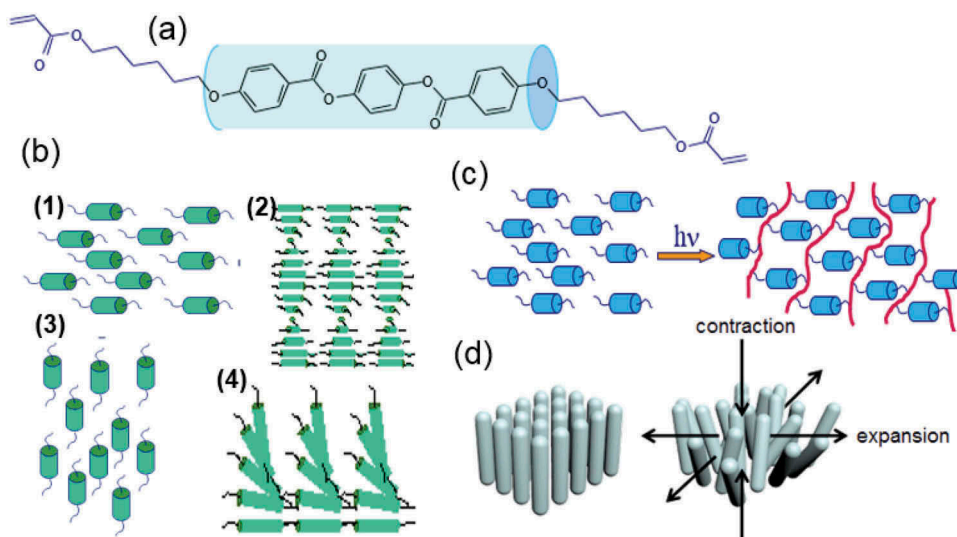


**Figure 1.** (colour online) Schematic illustration of the principle of LC. (a) An example of the molecule with reactive end groups. (b) Different types of alignment established at monomeric state. (c) Photo-polymerisation process to fix the nematic phase. (d) Anisotropic deformation of homeotropically aligned LCNs upon decreasing of the order.

optical properties of thin films and coatings are largely affected by the transformations in surface structure and shape. By controlling the surface topography, lens and grating structures can be formed in a dynamic and autonomous manner and their focusing depth might adapt to an external stimulus such as the light source itself and/or its directionality [5]. In relation to this, also appearance-related properties like scattering, diffraction or reflection can be modulated [6–8]. Furthermore, the wettability of the surface can be tuned between hydrophobic and hydrophilic or between hydrophilic and superhydrophobic states by forming and erasing the (sub)-micro surface reliefs [9,10].

Many studies are devoted to fabricate surface topographies by wrinkling, [11–14] lithography [15] or embossing [16–19]. A number of groups [20–23] have demonstrated the generation of surface relief gratings in thin films by using azobenzene-containing polymers. Gratings are fabricated by mass transport of polymer chains by continuous isomerisation of the azobenzene unit under a single beam of polarised light [24–26]. Most often, those structures are static after their formation. In this review, we elaborate on the methods and principles towards the creation of dynamic surface topographies at a coating on a confined substrate. These coatings can be switched between a flat state (in the absence of light of specific actuating wavelength) and a predesigned corrugated state through light illumination. The protrusions height correlates to the local volume increase verified by the density measurement as will be explained in the next section.

The use of liquid crystal polymer networks (LCNs) to induce the formation of surface topographies has been demonstrated to be a valuable approach to realise the above mentioned applications [27–30]. The principle of forming LCNs, and some examples of the molecular order, are provided in Figure 1. Figure 1(a) is a typical LC molecule that has an anisotropic shape with a rod-like stiff central core. It has two polymerisable end groups. In the monomeric state, various molecular configurations can be established as shown in Figure 1 (b): (1) uniaxial, (2) cholesteric (chiral-nematic), (3) vertically aligned or homeotropic and (4) splay-bend director patterns. There are several techniques to establish monolithic molecular order in LCs. For example, rubbed surfaces, surfactant treated surfaces, external electric or magnetic fields or flow can be applied. Occasionally, they are combined to create films of even more complex molecular architectures [31]. In fact, many LC alignment methods are developed for the display industry which all can be adapted for LC monomers. When the LC monomers are aligned in the desired order, photopolymerisation is initiated and the molecular orientation is in general preserved [32,33]. This results in a highly ordered LCN [34] as shown in Figure 1(c). Soft actuators based on LCNs that exhibit various morphing behaviour ranging from bending, curling to the more complex origami types of folding have been demonstrated by several groups [35–43]. In 2008, van Oosten and Warner have proposed the working mechanism of employing the glassy LCNs for morphing based on linear geometric expansions under the assumption of volume conservation. Upon

changing the degree of molecular order, both in number (order parameter) and in direction (director) position-dependent stresses are built up. These stresses lead to an anisotropic dimensional change of the LCNs, for example, with a contraction along the molecular orientation and expansions perpendicular to it (Figure 1(d)) while the total volume is unchanged.

## Volume increase

The theory explaining anisotropic linear expansion/contraction resulting in morphing of free-standing films could assist in explaining the phenomena observed during actuation of LCN coatings adhering to a solid substrate. However, a paradox was found when a uniform homeotropic film is confined on a rigid substrate. In the homeotropic configuration the mesogenic units are aligned perpendicularly to the substrate surface. In the presence of a copolymerised azobenzene molecule this LCN coating was mask exposed to UV light [44]. The isomerisation of azobenzene decreases the order of aligned LC molecules. Following the classical linear geometrical arguments, the coating should contract at the exposed places thus forming indents as could be derived from Figure 1(d). However, unlike predicted by the linear expansion theory, the exposed area does not form valleys; instead, protrusions are formed as shown in Figure 2. Given the fact that we are dealing with polymer networks, material mass transport to exposed area are unlikely to take place. The formation of the protrusions strongly suggests a density decrease and corresponding volume increase in the surface-constrained film and the linear expansion or contraction depending on the director direction does not, or to a far lesser extent, play a role. So it is postulated that the reduction of

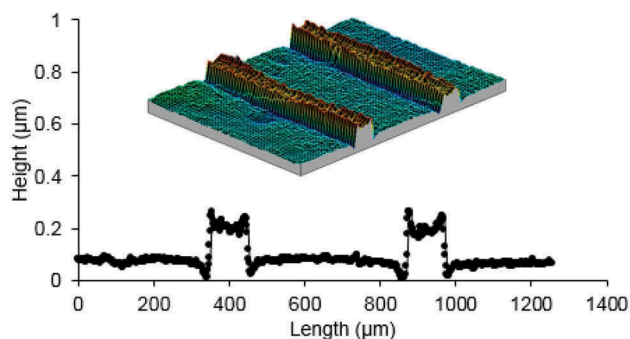


**Figure 2.** (colour online) Surface topographies of an azobenzene-modified homeotropic LCN coating during exposure through a line mask with a periodic pitch of 450  $\mu\text{m}$  and an opening of 100  $\mu\text{m}$ . The surface of the coating is analysed by interference microscope and displayed in 3D view and in cross-sectional view.

molecular order is accompanied with the density decrease (and corresponding volume increase), which is independent from the molecular alignment configurations [28]. Free volume formation in azobenzene side-chain polymers by photoactuation have been published earlier [45,46]. Barrett and co-workers reported even a volume increase of 17% at room temperature, measurements that were supported by neutron reflectometry. Here, the azobenzene content was much lower; 2% of the acrylate monomers units contain an azobenzene moiety versus 100% in the Barrett paper. Moreover, our experiments are at cross-linked polymer networks rather than with linear polymers. Free volume effects in free-standing bending films made of liquid crystal polymer networks were reported by the Ikeda and co-workers [47].

The foregoing experiment where the protrusions are formed in the homeotropically aligned LCNs indicates that the order parameter-related density decrease is more dominant than the arguments on order parameter-related linear geometrical change of dimensions. We verified this density decrease further. For this density, measurements were performed at free-standing films of the same composition in the exposed and in the non-exposed state. Prior to exposure, a density of 1.217  $\text{g}/\text{cm}^3$  at RT was measured by means of a density column. In a particular experiment the film was immersed in salt brine of the density of 1.202  $\text{g}/\text{cm}^3$  which makes the film sink, as demonstrated in Figure 3. Upon exposure with UV light the film starts floating, shown in Figure 3(b), indicating a density decrease. After switching off the light illumination the film sinks again (Figure 3(c-e)). Repeating this experiment by immersing this film in salt brine of different densities, but lower than that of the film, one could derive the density difference between exposed and non-exposed states.

The discovery of the density decrease has led to a new design of coatings in which order parameter-related anisotropic deformations and the excessive free volume effect can work together in concert. Guided by this philosophy, diverse surface topographic structures in thin coatings on rigid substrates were created [27–29]. Some examples are given in Figure 4. Figure 4(a) is a patterned film containing planar chiral-nematic areas next to homeotropic areas. Bringing two types of molecular order in one coating is realised by the use of patterned indium tin oxide (ITO) electrodes. The initially planar helicoidal molecular alignment can be locally unwound by the electric field. These two molecular alignments have opposite photomechanical response. In the planar chiral-nematic area, the reduction of the order parameter results in a positive expansion normal to the plane while the expansion in the homeotropic

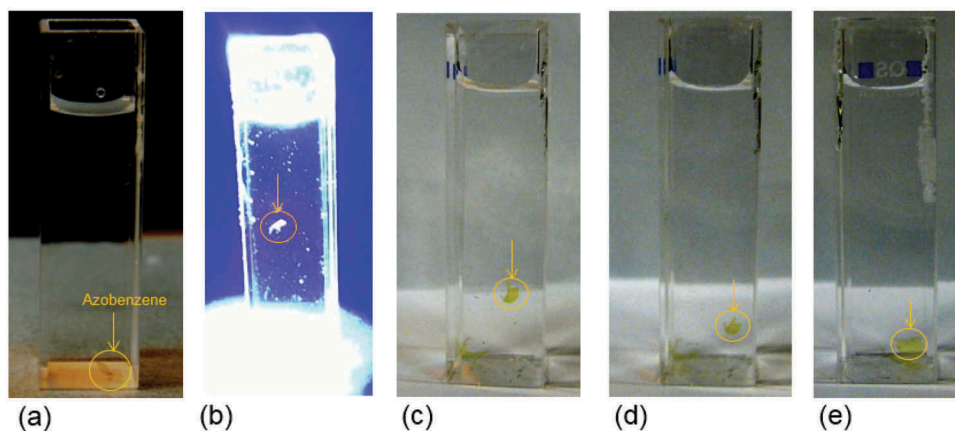


**Figure 3.** Density change in an azobenzene containing LC film. (a) Before UV exposure, the film is at the bottom of flask, (b) snapshot of films during exposure showing the film starts to float, and (c–e) after removing of UV light, the film sinks and reaches its initial position at the bottom.

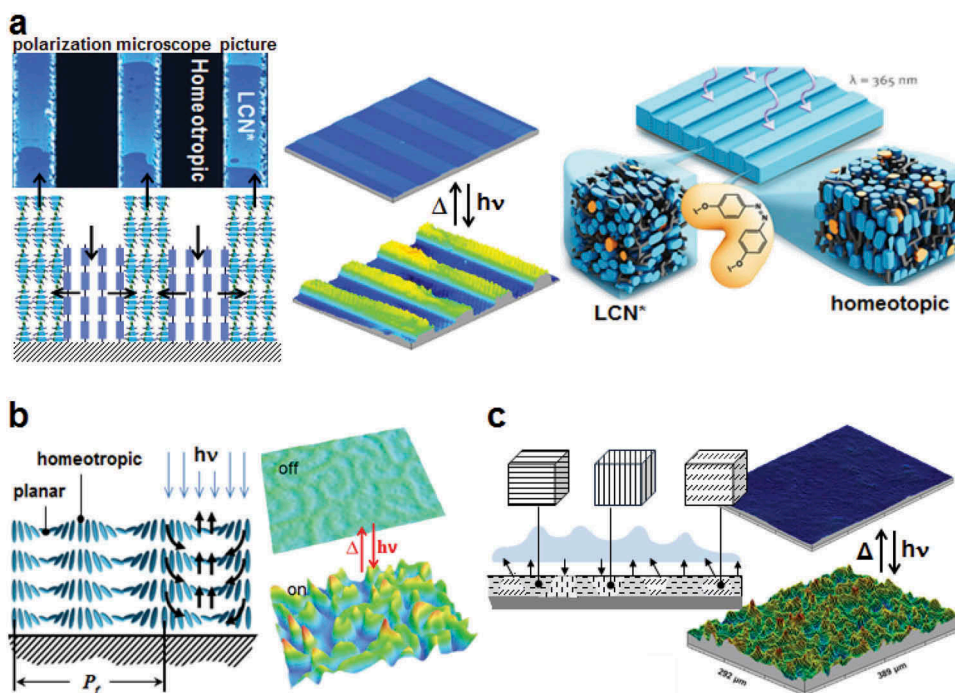


**Figure 4.** LCN coatings change their surface topology by UV actuation. (a) Coating with alternating stripes of chiral-nematic order LCN (LCN\*) and molecules aligned perpendicular to the substrate (homeotropic). Left: a polarisation microscope picture and schematic representation of the deformations upon actuation. Centre: interference microscopic images before and during deformation. Right: artistic impression of the deformation process. (b) When LCN\* helical axis are oriented parallel to the surface a fingerprint pattern is formed. Left: schematic representation of fingerprints deformation upon light actuation. Right: confocal microscopic measurement before and during actuation. (c) Dynamic surfaces formed at polydomain LCNs. Left: schematic representation of the deformations upon actuation. Right: interference microscopic measurement before and during actuation.

plane is close to zero or even negative. In the homeotropic area the opposite occurs when the molecular order is reduced it will undergo expansion within the plane of the film and contraction perpendicular to the film surface. This means that for patterned surfaces of sufficiently small dimensions the volume expansion is

assisted by the order parameter geometric effects. This combination of the two gives large deformations. The modulations depth, defined as  $\varphi = \left(\frac{Z_t}{Z_0}\right) \times 100\%$ , where  $Z_t$  is the height difference (depth) from peak to the valley of the adjacent profile,  $Z_0$  is the initial coating thickness, could reach values close to 20%.

In the foregoing experiment the helix axes in the planar area are normal to the substrate. Alternatively, the helix axes can be rotated 90 degrees as shown in [Figure 4\(b\)](#). This forms worm-like fingerprint textures which for some applications might provide several advantages. They are formed by a self-assembling process without involving lithographic procedures, unlike the method presented in [Figure 4\(a\)](#). Also the self-assembling process enables practical fabrication. But more importantly we could minimise the lateral protrusion dimensions from tens of micrometre to micrometres or smaller simply by adjusting the concentration of chiral monomeric molecules. Also, here the monomeric segments in the helices parallel to the surface tend to expand whereas the segments perpendicular to the surface tend to shrink. This leads to modulation depth between an 'on' and an 'off' state reaching the record value of 24% of the film thickness.

Although in the fingerprints method we can eliminate the lithographic patterning and the additional electric field to align the molecules, some efforts need to be devoted to balance the two distinct forces between the chiral force that rotates molecules along the helix axis and the anchoring force from substrate that tends to unwind the helix to a homeotropic alignment. To control this, the coating thickness must be of the order of half the periodicity of the molecular helix to form stable fingerprint textures. In order to make the dynamic surface topographies, a step forward to the potential applications a simple coating procedure was developed based on polydomain LCs. In polydomain LCs, molecules are aligned in discrete domain regions instead of over the entire coating area. Throughout the coating, domains are randomly distributed with various alignments ranging from uniaxial with different orientation direction in the plane of the layer, tilted with various tilt angles to domains with a (close to) homeotropic orientation. In each domain, molecules align differently without any preference for a specific orientation. Also, the domain sizes are varied along the coating if there are no additional forces involved. When the coating is exposed with light, each domain deforms differently. The planar regions form hills while the homeotropic areas expand less or can even deform into valleys when they can expand in the x-y plane when they are next to a planar region. Indeed when the homeotropic domain is next to a uniaxial domain, the highest tops are formed as they benefit from the lateral forces exerted by the homeotropic region. Due to the constraints from the substrate, and the interactions between domains with different LC alignments jagged surface topographies are formed as seen in [Figure 4\(c\)](#).

## Enhancement of volume increase

In the foregoing discussion, the photomechanical effect is induced by addressing the azobenzene with light of a wavelength that corresponds to the absorption band of its *trans* state. Recently, we discovered that free volume generation is enhanced by the oscillating dynamics of the *trans*-to-*cis* conversion of azobenzene [48]. This is stimulated even more by dual wavelength exposure promoting both excitation of *trans* and the *cis* isomer of azobenzene rather than populating *cis* isomer solely. This dynamics was proposed to be responsible for the lateral transport of azobenzene-modified side-chain polymers under the exposure with an interference pattern of a laser source [49]. Here, we anticipate its importance in our densely cross-linked networks where the dynamics in the azobenzene isomerisation enhances the formation of molecular voids in the polymer matrix resulting in a large volume increase on the macroscopic level. [Figure 5](#) shows this result. When a film is mask exposed to UV (365 nm) light at  $300 \text{ mW cm}^{-2}$  a local volume increase of just above 3% is obtained. Subsequently, when an additional LED lamp emitting at 455 nm light is directed to the same area a significant increase of the volume can be found which at optimised ratios reach values of almost 12%. Maximum density decreases are found when the 455 nm intensities is around 2.5%, 5% and 10% of the 365 nm intensities at 100, 200 and  $300 \text{ mW} \cdot \text{cm}^{-2}$ , respectively. At higher 365 nm intensity, a higher 455 nm intensity is needed to generate the maximum results. At higher 455 nm intensity the effect drops remarkably fast. It is also noteworthy that the effect at the higher 365 nm intensity of  $300 \text{ mW} \cdot \text{cm}^{-2}$  is disproportional larger than measured at the lower 365 nm intensity experiments. From here we conclude that the conversion of the *trans* azobenzene to its photostationary *cis* state is not the main factor that generate large free volume. Instead, the activation of the back reaction from *cis* to *trans* plays a dominant role. To verify this theory further, a small amount of fluorescence dye was added that absorbs 365 nm light and emits blue light into the coating. In this case, just a single wavelength exposure at 365 nm light is sufficient. The results show a much larger volume formation than without dye.

Because free volume is thermodynamically highly unfavourable, this out of equilibrium effect leads to a fast relaxation of the surface as soon as UV trigger stops within tens of seconds. It is in fact much faster than pre-described by chemical relaxation of the photochemical azobenzene compound that is several hours [50].

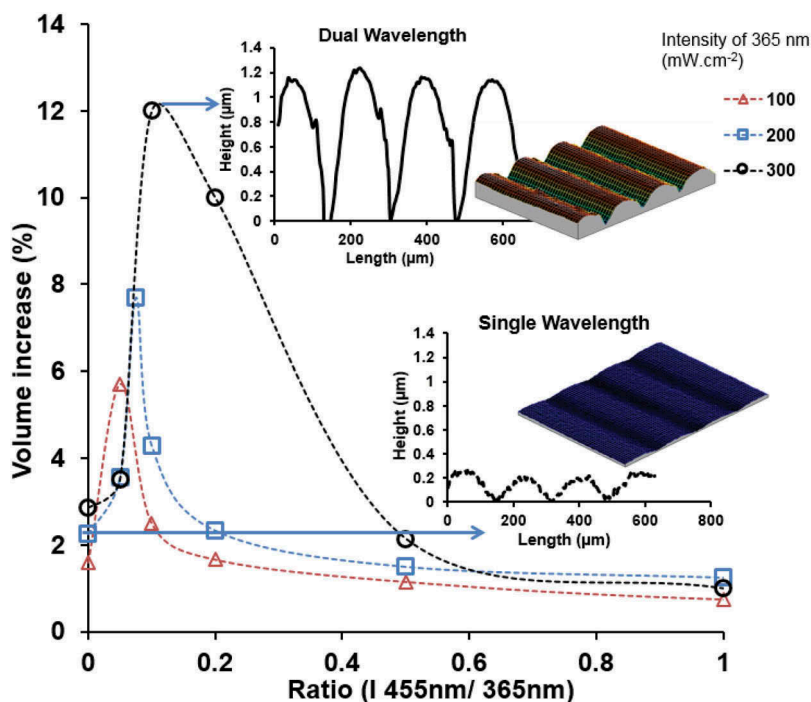


**Figure 5.** (colour online) Density decrease of LCN\* under the different illumination conditions. 365 nm LED light with various intensities:  $100 \text{ mW} \cdot \text{cm}^{-2}$  (red line),  $200 \text{ mW} \cdot \text{cm}^{-2}$  (blue line), and  $300 \text{ mW} \cdot \text{cm}^{-2}$  (black line) is mixed with 455 nm LED light (red line). Inset shows interference microscopy measurements of surface topographies when exposure to single 365 nm light (3D image and the corresponding surface profile), and exposure to dual 365 and 455 nm light (3D image and its surface profile).

## Conclusions

In this review, several methods towards the creation of dynamic surface topographies in liquid crystal polymer thin coatings are described. Integrated with azobenzene molecules, these glassy coatings can be switched between a flat state (in dark) and a predesigned corrugated state through light illumination. The driving force for the formation of the surface topographies is a density decrease/volume increase upon the order parameter reduction. Unlike when being studied in an LC elastomer, the azobenzene, though present in a very small amount of less than 5 w%, is able to create free volume by which the density of the polymer decreases up to 10%. Furthermore, it is found that to amplify this process the molecular dynamics of the *trans*-to-*cis* isomerisation reaction overrules the actual conversion to the *cis* state contradicting with the current theories of photo-actuation. The photoresponsive effect can be largely enhanced by simultaneously light triggering both the *trans* and the *cis* state of the molecule. This can be realised by either focusing two light beams with 365 nm and 455 nm wavelength or adding a small concentration of fluorescent dye absorbs 365 nm light while emitting 455 nm light.

Dynamic surface topographies give an entrance to new applications of these materials ranging from self-

cleaning, friction control, opto-photonics to haptics, touch sensation and micro-robotics, just because of the sizable surface effects.

## Disclosure statement

No potential conflict of interest was reported by the author.

## Funding

The results presented are part a research programme financed by the Dutch Polymer Institute (DPI) [project # 775].

## References

- [1] Meijer HEH, Singh MK, Kang TG, et al. Passive and active mixing in microfluidic devices. *Macromol Symp.* 2009;279:201–209. doi:10.1002/masy.v279:1.
- [2] Mavroidis C, Pfeiffer C, Celestino J, et al. Fabrication of a robotic hand using rapid prototyping. 26th Biennial Mechanisms and Robotics Conference; 2000 Sep 10–13, Baltimore, MD.
- [3] Wakuda M, Yamauchi Y, Kanzaki S, et al. Effect of surface texturing on friction reduction between ceramic and steel materials under lubricated sliding contact. *Wear.* 2003;254:356–363. doi:10.1016/S0043-1648(03)00004-8.

- [4] Pettersson U, Jacobson S. Textured surfaces for improved lubrication at high pressure and low sliding speed of roller/piston in hydraulic motors. *Tribol Int.* 2007;40:355–359. doi:10.1016/j.triboint.2005.11.024.
- [5] Dong L, Agarwal AK, Beebe DJ, et al. Adaptive liquid microlenses activated by stimuli-responsive hydrogels. *Nature.* 2006;442:551–554. doi:10.1038/nature05024.
- [6] De Jong TM, De Boer DKG, Bastiaansen CWM. Surface-relief and polarization gratings for solar concentrators. *Opt Express.* 2011;19:15127–15142. doi:10.1364/OE.19.015127.
- [7] Schiff H, Halbeisen M, Schütz U, et al. Surface structuring of textile fibers using roll embossing. *J Microelectron Eng.* 2006;83:855–858. doi:10.1016/j.mee.2006.01.120.
- [8] Ibn-Elhaj M, Schadt M. Optical polymer thin films with isotropic and anisotropic nano-corrugated surface topologies. *Nature.* 2001;410:796–799. doi:10.1038/35071039.
- [9] Li C, Zhang Y, Ju J, et al. In situ fully light-driven switching of superhydrophobic adhesion. *Adv Funct Mater.* 2012;22:760–763. doi:10.1002/adfm.201101922.
- [10] Onda T, Shibuichi S, Satoh N, et al. Super-water-repellent fractal surfaces. *Langmuir.* 1996;12:2125–2127. doi:10.1021/la950418o.
- [11] Kim J, Hanna JA, Byun AM, et al. Designing responsive buckled surfaces by halftone gel lithography. *Science.* 2012;335:1201–1205. doi:10.1126/science.1215309.
- [12] Kim J, Hanna JA, Hayward RC, et al. Thermally responsive rolling of thin gel strips with discrete variations in swelling. *Soft Matter.* 2012;8:2375–2381. doi:10.1039/c2sm06681e.
- [13] Stoychev G, Pureskiy N, Ionov L. Self-folding all-polymer thermoresponsive microcapsules. *Soft Matter.* 2011;7:3277–3279. doi:10.1039/c1sm05109a.
- [14] Klein Y, Efrati E, Sharon E. Shaping of elastic sheets by prescription of non-euclidean metrics. *Science.* 2007;315:1116–1120. doi:10.1126/science.1135994.
- [15] Xia Y, Whitesides GM. Soft lithography. *Angew Chem Int Ed.* 1998;37:550–575. doi:10.1002/(SICI)1521-3773(19980316)37:5<550::AID-ANIE550>3.0.CO;2-G.
- [16] Berendsen CWJ, Škerek M, Najdek D, et al. Superhydrophobic surface structures in thermoplastic polymers by interference lithography and thermal imprinting. *Appl Surf Sci.* 2009;255:9305–9310. doi:10.1016/j.apsusc.2009.07.001.
- [17] Hermans K, Tomatsu I, Matecki M, et al. Highly efficient surface relief formation via photoembossing of a supramolecular polymer. *Macromol Chem Phys.* 2008;209:2094–2099. doi:10.1002/macp.200800355.
- [18] Sánchez C, De Gans BJ, Kozodaev D, et al. Photoembossing of periodic relief structures using polymerization-induced diffusion: A combinatorial study. *Adv Mater.* 2005;17:2567–2571. doi:10.1002/adma.200500777.
- [19] Paul KE, Breen TL, Aizenberg J, et al. Maskless photolithography: embossed photoresist as its own optical element. *App Phys Lett.* 1998;73:2893–2895. doi:10.1063/1.122621.
- [20] Viswanathan NK, Balasubramanian S, Li L, et al. Surface-initiated mechanism for the formation of relief gratings on azo-polymer films. *J Phys Chem B.* 1998;102:6064–6070. doi:10.1021/jp981425z.
- [21] Barrett CJ, Natansohn AL, Rochon P. Mechanism of optically inscribed high-efficiency diffraction gratings in azo polymer films. *J Phys Chem.* 1996;100:8836–8842. doi:10.1021/jp953300p.
- [22] Liu B, Wang M, He Y, et al. Duplication of photoinduced azo polymer surface-relief gratings through a soft lithographic approach. *Langmuir.* 2006;22:7405–7410.
- [23] Critsai Y, Goldenberg LM, Stumpe J. Efficient single-beam light manipulation of 3D microstructures in azobenzene-containing materials. *Opt Express.* 2011;19:18687–18695.
- [24] Pedersen TG, Johansen PM, Holme NCR, et al. Mean-Field theory of photoinduced formation of surface reliefs in side-chain azobenzene polymers. *Phys Rev Lett.* 1998;80:89–92. doi:10.1103/PhysRevLett.80.89.
- [25] Ichimura K. Photoalignment of liquid-crystal systems. *Chem Rev.* 2000;100:1847–1874. doi:10.1021/cr980079e.
- [26] Natansohn A, Rochon P. Photoinduced motions in azo-containing polymers. *Chem Rev.* 2002;102:4139–4176. doi:10.1021/cr970155y.
- [27] Liu D, Bastiaansen CWM, den Toonder JMJ, et al. Photo-switchable surface topologies in chiral nematic coatings. *Angew Chem Int Ed.* 2012;51:892–896. doi:10.1002/anie.201105101.
- [28] Liu D, Bastiaansen CWM, den Toonder JMJ, et al. Light-induced formation of dynamic and permanent surface topologies in chiral-nematic polymer networks. *Macromolecules.* 2012;45:8005–8012. doi:10.1021/ma301628h.
- [29] Liu D, Broer DJ. Self-assembled dynamic 3D fingerprints in liquid-crystal coatings towards controllable friction and adhesion. *Angew Chem Int Ed.* 2014;53:4542–4546. doi:10.1002/anie.201400370.
- [30] Liu D, Liu L, Onck PR, et al. Reverse switching of surface roughness in a self-organized polydomain liquid crystal coating. *PNAS.* 2015;112:3880–3885. doi:10.1073/pnas.1419312112.
- [31] Broer DJ. Creation of supramolecular thin film architectures with liquid-crystalline networks. *Mol Liq Cryst.* 1995;261:513–523. doi:10.1080/10587259508033494.
- [32] Kitzrow H-S, Schmid H, Ranft A, et al. Observation of blue phases in chiral networks. *Liq Cryst.* 1993;14:911–916. doi:10.1080/02678299308027768.
- [33] Broer DJ, Heynderickx I. Three-dimensionally ordered polymer networks with a helicoidal structure. *Macromolecules.* 1990;23:2474–2477. doi:10.1021/ma00211a012.
- [34] Broer DJ, Crawford GP, Zumer S editor. Cross-linked liquid crystalline systems: from rigid polymer networks to elastomers. Boca Raton, FL: CRC Press Taylor and Francis Group; 2011.
- [35] Yu H, Ikeda T. Photocontrollable liquid-crystalline actuators. *Adv Mater.* 2011;23:2149–2180. doi:10.1002/adma.v23.19.
- [36] Schenning APHJ, Bastiaansen CWM, Broer DJ, et al. The role of supramolecular chemistry in stimuli responsive and hierarchically structured functional organic materials. *Chim Oggi.* 2014;32:78–80.
- [37] Evans JS, Ackerman PJ, Broer DJ, et al. Smalyukh II. Optical generation, templating, and polymerization of



- three-dimensional arrays of liquid-crystal defects decorated by plasmonic nanoparticles. *Phys Rev E*. 2013;87:032503. doi:10.1103/PhysRevE.87.032503.
- [38] Warner M, Modes CD, Corbett D. Curvature in nematic elastica responding to light and heat. *Proc R Soc A*. 2010;466:2975–2989. doi:10.1098/rspa.2010.0135.
- [39] Camacho-Lopez M, Finkelmann H, Palffy-Muhoray P, et al. Fast liquid-crystal elastomer swims into the dark. *Nat Mater*. 2004;3:307–310. doi:10.1038/nmat1118.
- [40] White TJ, Serak SV, Tabiryan NV, et al. Polarization-controlled, photodriven bending in monodomain liquid crystal elastomer cantilevers. *J Mater Chem*. 2009;19:1080–1085. doi:10.1039/B818457G.
- [41] van Oosten CL, Bastiaansen CWM, Broer DJ. Printed artificial cilia from liquid-crystal network actuators modularly driven by light. *Nat Mater*. 2009;8:677–682. doi:10.1038/nmat2487.
- [42] Kosa T, Sukhomlinova L, Su L, et al. Light-induced liquid crystallinity. *Nature*. 2012;485:347–349. doi:10.1038/nature11122.
- [43] Yu Y, Nakano M, Ikeda T. Photomechanics: directed bending of a polymer film by light. *Nature*. 2003;425:145–145. doi:10.1038/425145a.
- [44] Liu D. Responsive surface topographies [PhD thesis]. Eindhoven: Technische Universiteit Eindhoven; 2013. ISBN: 978-90-386-3317-6.
- [45] Yager KG, Tanchak OM, Godbout C, et al. Photomechanical effects in azo-polymers studied by neutron reflectometry. *Macromolecules*. 2006;39:9311–9319. doi:10.1021/ma0617320.
- [46] Mechau N, Saphiannikova M, Neher D. Dielectric and mechanical properties of azobenzene polymer layers under visible and ultraviolet irradiation. *Macromolecules*. 2005;38:3894–3902. doi:10.1021/ma0479316.
- [47] Priimagi A, Shimamura A, Kondo M, et al. Location of the azobenzene moieties within the cross-linked liquid-crystalline polymers can dictate the direction of photo-induced bending. *ACS Macro Lett*. 2012;1:96–99. doi:10.1021/mz200056w.
- [48] Liu D, Broer DJ. New insights into photoactivated volume generation boost surface morphing in liquid crystal coatings. *Nat Comm*. 2015;6:8334. doi:10.1038/ncomms9334.
- [49] Vapaavuori J, Goulet-Hanssens A, Heikkinen ITS, et al. Are two azo groups better than one? investigating the photoresponse of polymer-bisazobenzene complexes. *Chem Mater*. 2014;26:5089–5096. doi:10.1021/cm5023129.
- [50] Kumar GS, Neckers DC. Photochemistry of azobenzene-containing polymers. *Chem Rev*. 1989;89:1915–1925. doi:10.1021/cr00098a012.